A soluble model of domain growth in one-dimensional disordered systems

1993 J. Phys. A: Math. Gen. 26 5237

(http://iopscience.iop.org/0305-4470/26/20/011)

J. Phys. A: Math. Gen. 26 (1993) 5237–5254. Printed in the UK

A soluble model of domain growth in one-dimensional disordered systems

R E Blundell and A J Bray
Department of Theoretical Physics, The University, Manchester M13 9PL, UK

Received 14 May 1993

Abstract. We introduce a new algorithm for domain growth in disordered systems at low temperatures based on the tendency for such a system to freeze into metastable states. We apply the algorithm to the $d = 1$ random-bond Ising model for a variety of bond distributions. The analytical forms we obtain for the two-point correlation function and autocorrelation function agree well with numerical simulations of the model. These forms are not the same as those of the pure Ising model with Glauber dynamics.

1. Introduction

The properties of domain growth in systems quenched from a disordered state to a temperature within the ordered phase have been extensively investigated [1]. Interest has focused on the nature of the growth law for the characteristic scale $L(t)$ and on the form of the scaling function $f(x)$ for the two-point correlation function $C(x) = f(r/L(t)) = f(x)$. For systems without disorder, it has been shown that $L(t) \sim t^n$ where the growth exponent n is known both for conserved ($n = \frac{1}{3}$) and non-conserved ($n = \frac{1}{2}$) order parameters [2, 3]. The scaling function $f(x)$, however, has proved difficult to calculate exactly for physically interesting values of d [4] although approximate theories have been developed which give reasonable agreement with numerical simulations for scalar [5] and vector [6] (non-conserved) order parameters.

Considerably less progress has been made in the study of disordered systems. Analytical results have been limited. Huse and Henley [7] have argued that the characteristic length scale grows as $L(t) \sim (\log(t))^x$ where the exponent x is related to the static exponents governing the pinning energy and the domain wall roughening. Numerical simulations using Monte Carlo algorithms or cell dynamics are hampered by the freezing of the spins in metastable configurations [8, 9]. Recent results for the growth law for the characteristic length scale using cell dynamics, however, are consistent with the prediction of Huse and Henley of the growth law for the characteristic scale $L(t)$ for both conserved and non-conserved order parameters although it is still not clear whether the asymptotic regime has been reached.

The scaling functions for the two-point correlation function and autocorrelation function have not been calculated analytically and the approximate theories mentioned above have not proved adaptable to disordered systems. It has been suggested, however, that although the introduction of disorder roughens the domain walls, on a sufficiently coarse grained scale the walls appear smooth such that domain growth is driven by the curvature of the walls on large scales [10]. Simulation results for the two-point correlation function and

0305-4470/93/205237+18$07.50

autocorrelation function of the $d = 2$ random-bond Ising model (RBIM) appear to confirm this prediction (Bray and Humayun, [8]). The scaling function found, expressed in terms of the length scale $L(t)$, appears to be the same as for pure systems.

In view of the difficulties associated both with analytical work and numerical simulation of phase ordering in disordered systems it would seem useful to consider a model which can be solved exactly. In this paper we present a new algorithm for domain growth which exploits the tendency of the system to freeze into metastable configurations at low temperatures. Although in principle the algorithm is applicable to any disordered system, it proves impractical to implement other than in one dimension.

A disordered system of particular interest in $d = 1$ is the RBIM. Unlike the Ising model in a random field, the disorder does not destabilize the ground state and so a transition to an ordered state occurs, albeit at zero temperature. We have used our algorithm to simulate this model and hence determined the form of the two-point correlation function and autocorrelation function for a variety of bond distributions. In certain cases we have also been able to deduce these functions analytically, and in these cases the fit to the numerical data is excellent. Our solution satisfies the dynamic scaling hypothesis, which states that the domain morphology is characterised by a single time-dependent length scale. Interestingly, the results obtained are not the same as the corresponding quantities in the $d = 1$ Glauber model, i.e. the same system without disorder [4].

The time dependence of the characteristic length scale $L(t)$ can be deduced rather simply for these models. It is convenient, however, to express the scaling functions in terms of L_0, the average domain scale, so the correlation functions we calculate are of the form $C \sim f(r/L_0)$. In this form the scaling functions exhibit a degree of universality. For example, the function $f(x)$ is the same for all unbounded distributions of bonds. By contrast, the dependence of L_0 on t depends on the details of the distribution. This will be discussed in more detail in section 6.

The rest of this paper is organized as follows. A general definition of the model is presented in section 2. A more detailed explanation of how the model is applied numerically to the RBIM is given in section 3. When the bond distribution is unbounded the calculation of the scaling function $f(x)$ for the two-point correlation function becomes rather straightforward. Section 4 contains a calculation of this quantity along with a similar but more involved calculation for a uniform distribution of bonds. In section 5 we discuss the form of the autocorrelation function for an unbounded distribution of bonds. The results are discussed and summarized in section 6.

2. The model

Consider the evolution of order in a system with some form of random disorder, and a discrete spin symmetry, quenched from the high-temperature phase. Initially the ordering occurs rapidly but the system soon becomes trapped in a metastable configuration. If the temperature is very low, then on the time scale of the initial ordering the system will remain in this state virtually indefinitely. On a longer time scale, however, excitations cause the system to move to new metastable states with lower energies and hence the system moves towards equilibrium.

The idea of our algorithm is to exploit two properties of domain ordering in random systems at low temperature: firstly the tendency of the system to spend most of its time in metastable states and secondly the increasing differentiation, as $T \to 0$, of the time scales associated with the occurrence of processes with different excitation energies.

The time scale on which an excitation away from a metastable state occurs is determined

by both its energy cost and a factor associated with the number of paths through phase space by which the target state can be reached from the metastable configuration in which the system is frozen. In the limit of very low temperature the energy cost becomes the dominant factor, so that excitations with lower energy costs occur far more frequently, and hence sooner, than those with higher ones. Most excitations have no effect because the system quickly relaxes back to the original state. For certain excitations, however, relaxation to another metastable configuration with a lower energy is possible and hence their presence determines the dynamics of the system.

The path the system follows through phase space is determined, therefore, by the energy of the excitations required to move it from one metastable configuration to another. At sufficiently low temperature the configuration to which the system moves is the one that requires excitation with the smallest energy cost. The essential idea of our algorithm is that for small T the time scales of the various excitations become increasingly differentiated and as $T \to 0$ only the fastest processes need be considered. One can therefore determine, in principle at least, the states through which the system passes by calculating the energy barriers involved in moving the system between metastable states and choosing as the new state the one with the smallest energy barrier. In practice, for most systems the number of possible excitations leading to new metastable states is too large to cope with. For a one-dimensional system, however, the situation is much simpler and it is possible in certain cases to implement the algorithm numerically and to deduce the late-time domain structure analytically.

We believe that at sufficiently low temperature our algorithm is equivalent to Monte Carlo dynamics and should produce the same spin configurations. We note, however, that a given step of the algorithm corresponds to a varying number of steps of the underlying Monte Carlo dynamics, so we cannot sensibly define time as the number of iterations. Instead, we use the average domain size, simply the reciprocal of the domain wall density in $d = 1$, to define a characteristic length with which to scale the correlation function etc. The form of the growth law for the characteristic scale, expressed in terms of the equivalent Monte Carlo time, is discussed in section 6. Note that an actual Monte Carlo simulation is not practical because of the enormous time scales required to grow domains of size comparable to those produced by the new algorithm.

3. The random-bond Ising model in one dimension

For the $d = 1$ RBIM we are able to calculate the correlation function exactly for an unbounded or a uniform distribution of bonds. Before we present these calculations, however, we shall explain more precisely how the general algorithm outlined above applies to the $d = 1$ RBIM and in particular how we have implemented it numerically.

It is simpler to consider the dynamics of the domain walls (interfaces) rather than the dynamics of the individual spins. The interfaces lie on the dual lattice to the spins and have a creation energy equivalent to the strength of the bond that they break. We can therefore think of the bonds as defining a energy surface on which the interfaces move. Because of the disorder, this surface has many local minima.

After a few steps of normal Glauber dynamics the interfaces will become stuck in these local minima. To implement our algorithm we take each interface in turn and compute the first position to the left and to the right which has a lower energy, i.e. which is the site of a weaker bond and which is also a local minimum. Transitions to states with a higher energy need not be considered because the energy barrier for the return to the original state is necessarily lower than the barrier to the high energy state, so for $T \to 0$ the system

spends a negligible fraction of time in the high energy state. We next find the largest bond between the interface site and the target site. The difference between this bond and the bond on which the interface sits is the energy barrier for moving the interface to the new site. Having evaluated the energy barriers for the movement of all the interfaces, we find the smallest one and move the corresponding interface to its new position. If this site is already occupied by an interface, then both interfaces are eliminated from the system. Note that there cannot be any interfaces between as they would have already been moved due to their smaller energy barriers.

The size of the energy barrier that can be jumped by an interface defines a time scale. The larger the barrier, the longer we expect to wait before the interface jumps over it. At a particular stage of the ordering process there will be a maximum barrier size that has been jumped by any interface. Because our algorithm relies on the temperature being very low, the time scale associated with this barrier will be very much greater than that associated with the next largest barrier so we should therefore regard all processes that require the jumping of barriers less than the maximum jumped so far as instantaneous on this time scale. When we wish to observe the state of the system, say to calculate the correlation function, we therefore ensure that all processes requiring the jumping of barriers less than the current maximum are completed.

We have ignored the effects of interface creation in this procedure. At the earliest stages this is not a problem, because to create an interface requires the breaking of two bonds, which will be a higher energy cost than that needed to move an interface, which involves only a change in which bonds are broken. At late stages, however, the size of the energy barriers to interface motion will have increased to the point where the production of interfaces is less costly energetically than the jumping of the barriers. On the time scale required to jump a barrier, therefore, there will be many interface pairs created. These new interfaces have no effect on the domain structure, however, because they cannot jump any of the large remaining barriers. They are therefore confined in pairs to the regions between the barriers and quickly annihilate with one another. The fraction of time in a true Monte Carlo study that these interfaces would be present is negligible and therefore their effect on the the measured values of the correlation functions can be ignored.

Numerical implementation of the above procedure is straightforward. Starting from a random spin configuration, we run a normal Monte Carlo simulation, based on Glauber dynamics at $T = 0$, until the entire set of spins is frozen. Given this configuration of spins, we then start our algorithm as defined above. We have run simulations for a variety of random bond distributions. Figure 1 shows the correlation function found for a power-law distribution of bonds defined by the probability density $P(J) = (\alpha - 1)J^{-\alpha}\theta(J - 1)$, where $\theta(x)$ is the step function, along with the analytical form derived below. We have included data from a single time and only for the case $\alpha = 1.3$. Data taken at other times and from runs using different values of α all lie on the same curve however. Figure 2 shows the correlation function found when the distribution of bonds is uniform. Because we are working in $d = 1$ we are able to use large lattice sizes ($N = 10^5$) which eliminates any finite size effects. We are also able to reach rather large domain sizes ($L \sim 200$) and hence we are confident that the system has reached the asymptotic scaling regime. The data appear to scale well after the domain size exceeds about 50 for the broadest distributions although other distributions take longer to reach the scaling regime. It is interesting to note that the pure $d = 1$ Ising model with Glauber dynamics approaches the scaling limit considerably faster than this. The data for different power-law distributions of bonds and for an exponential distribution appear to give the same scaling function. We expect, in fact, that all unbounded distributions of bonds will give this scaling function. We return to this

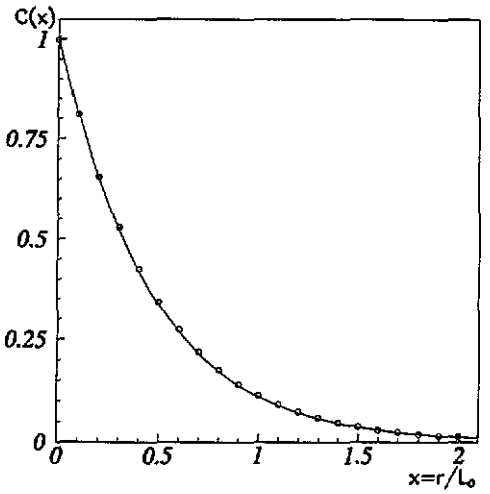

Figure 1. Scaling function for the two-point correlation function of the $d = 1$ random-bond Ising model with a power law distribution of bonds $P(J)$ as defined in the text with $\alpha = 1.3$. The solid line is the analytical prediction and the data points come from a numerical simulation of 200 realizations of 10^5 spins. The data were taken when the average domain size was $L_0 = 200$. The data for other values of L_0 and α, as well as the data for an exponential distribution of bonds, lie on the same curve.

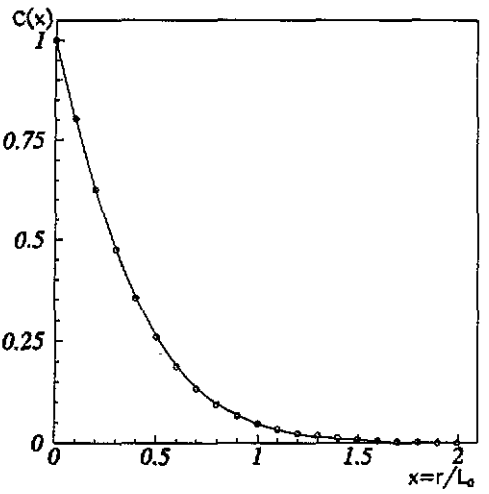

Figure 2. Scaling function for the two-point correlation function of the $d = 1$ random-bond Ising model with a uniform distribution of bonds. The solid line is the analytical prediction and the data points come from a numerical simulation of 200 realizations of 10^5 spins. The data were taken when the average domain size was $L_0 = 200$.

contention below.

We now turn to the calculation of the two-point correlation function, firstly in the case where the bonds come from an unbounded distribution, and then for the case where the distribution is uniform.

4. Calculation of the correlation function

4.1. Unbounded distribution of bonds

When the distribution of bonds is unbounded we can make a useful simplification of the problem. The size of an energy barrier depends on the difference between the bond which an interface breaks and the largest bond between this bond and the nearest weaker bond. For a distribution of bonds with an unbounded tail, the variation in the size of the large bond is the dominant factor in deciding the energy barrier because in a large domain the smallest bond tends to be very close to the minimum of the bond distribution. We can therefore ignore the distribution of the small bonds and concentrate on the locations of the large bonds. We will justify this simplification below when what we need to assume becomes clearer.

Consider the structure of the domains at late times. The maximum energy barrier that has been jumped will be large, hence the number of bonds sufficiently strong to be barriers to interface movement will be small. Interfaces in a region between two of these bonds will have been free to move provided these bonds are not broken. These interfaces consequently

will have annihilated with each other until the number remaining is either zero or one depending on the initial number of interfaces in the region. If the initial state of each spin is random, corresponding to infinite temperature, the probability of finding an interface at a given site is $\frac{1}{2}$, so the probability of an even or odd number of interfaces in a given region is also $\frac{1}{2}$. From this information we can deduce the structure of the spin configuration as follows: The spatial distribution of bonds sufficiently strong to form a barrier is a Poisson distribution because the occurrence of these bonds is a rare event. Between any two strong bonds there is an interface with probability $\frac{1}{2}$ which, if present, lies predominantly on the smallest bond, the expected position of which is uniformly distributed between the bonds. These observations reduce the calculation of the two-point correlation function, or indeed other correlation functions, to a combinatorial problem which can be solved exactly.

To calculate the two-point correlation function we take two points at a given separation and average over all realizations of initial conditions and disorder. This calculation can be further simplified by the following observation. Consider the situation where the points are separated by a region containing two strong bonds (by strong bonds we mean bonds sufficiently large to create a barrier to interface motion). Between these bonds there is an interface with probability $\frac{1}{2}$. This configuration consequently gives no contribution to the correlation function, because, when we average over initial conditions, we give equal weight to the configurations containing an interface between the large bonds and those that do not. These configurations give opposite contributions and therefore cancel. This cancelation occurs whenever there is the possibility of an interface between the points. We therefore define a potential interface (PI) to be a bond which, when the initial conditions are averaged out, is broken by an interface with probability $\frac{1}{2}$. Any configuration where the points are separated by a PI gives no contribution to the correlation function, so the correlation function is simply the probability that there is no PI between the two points.

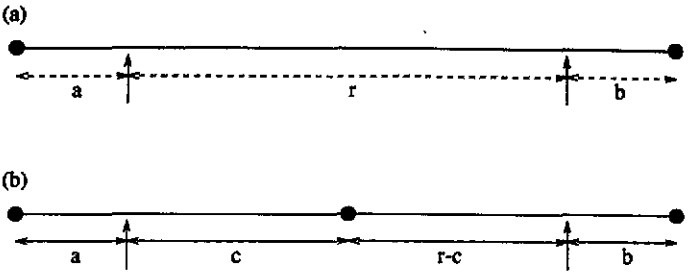

Figure 3. (*a*), (*b*) Configurations contributing to the two-point correlation function for the RBIM with an unbounded distribution of bonds. The large dots represent the positions of the strong bonds and the arrows the position of the points for which the correlation function is to be calculated. See the text for details.

Let us first consider the situation where the points have no strong bonds between them. The points lie in a region between two strong bonds as shown in figure 3(*a*). The PI associated with the strong bonds is located at the smallest bond between them, the position of which is uniformly distributed. To calculate the contribution to the correlation function from this configuration we sum over all positions of the strong bonds that place them outside the test points and include two factors in the sum: One for the probability of finding the strong bonds in these positions and one for the probability that the PI, i.e. the weakest bond, is not between the test points. In the scaling limit, the domain size is very much greater than the lattice spacing and so we can treat the model in the continuum limit. If we define the probability of finding a strong bond in an infinitesimal range of size da to be P_Sda then

the probability of the strong bond configuration shown in figure 3(*a*) is, from elementary probability theory, $P_S^2 \exp(-P_S(r+a+b))\mathrm{d}a\mathrm{d}b$. The probability that the PI lies outside the test points is $(a+b)/(a+b+r)$. The contribution to the correlation function from this configuration is therefore

$$P_S^2 \int_0^\infty \mathrm{d}a \int_0^\infty \mathrm{d}b \, \frac{(a+b)\exp(-P_S(r+a+b))}{a+b+r} . \tag{1}$$

The contribution from the situation in which there is one strong bond between the test points can be calculated in the same manner. We need to sum over all positions the strong bond between the points can take and include a factor that requires both PIs to lie outside the points (see figure 3(*b*)). This gives the expression

$$P_S^3 \int_0^\infty \mathrm{d}a \int_0^\infty \mathrm{d}b \int_0^r \mathrm{d}c \, \frac{ab\exp(-P_S(r+a+b))}{(a+c)(b+r-c)} . \tag{2}$$

We now turn to the evaluation of the integrals. If the rescaling $c' = rc$ is made in the c integral in (2) then r and P_S occur only in the combination rP_S and hence the scaling limit is defined by $r \to \infty$, $P_S \to 0$ with $rP_S = 2x$ arbitrary. The average separation of strong bonds is $1/P_S$ as their positions come from a Poisson distribution hence the average separation of interfaces is $2/P_S$ which is the same as the domain scale L_0. It follows therefore that $x = r/L_0$. It is more convenient, however, to calculate the two-point correlation function in the form $C(rP_S) = C(x/2)$ rather than $C(x)$. Normally the comparison of theoretical and simulation results requires a free parameter to be introduced because the definitions of the characteristic length scale differ. We can eliminate P_S in favour of L_0, however, and hence compare directly with the numerical simulations.

Taking the scaling limit in the above expressions gives

$$C(x/2) = \int_0^\infty \mathrm{d}a \int_0^\infty \mathrm{d}b \, \exp(-x(a+b+1))\left[\frac{x^2(a+b)}{a+b+1} + \int_0^1 \mathrm{d}c \, \frac{x^3ab}{(a+c)(b+1-c)}\right] . \tag{3}$$

To simplify this expression we write the denominators as integrals of exponentials which gives

$$C(x/2) = \int_0^\infty \mathrm{d}a \int_0^\infty \mathrm{d}b \int_0^\infty \mathrm{d}u \left[x^2(a+b)\exp(-(u+x)(a+b+1)) + \int_0^\infty \mathrm{d}v \int_0^1 \mathrm{d}c \, x^3ab\exp(-x(a+b+1)-u(a+c)-v(b+1-c))\right] . \tag{4}$$

After evaluating the integrals over a, b and c we have

$$C(x/2) = \int_0^\infty \mathrm{d}u \, \frac{2x^2\exp(-(u+x))}{(u+x)^3} + \int_0^\infty \mathrm{d}v \int_0^\infty \mathrm{d}u \, \frac{2x^3\exp(-x-v)}{(x+u)^2(x+v)^2(u-v)} . \tag{5}$$

Using the identity

$$\int_0^\infty \mathrm{d}u \, \frac{1}{(x+u)^2(u-v)} = \frac{-1}{x(x+v)} + \frac{1}{(x+v)^2}\ln\left(\frac{x}{v}\right) \tag{6}$$

gives, after a little manipulation, the single integral

$$C(x) = \int_0^1 \mathrm{d}v \, 2v^2\exp\left(-\frac{2x}{v}\right)\ln\left(\frac{v}{1-v}\right) \tag{7}$$

which is our final form for the correlation function. The same expression can also be derived without using the continuum form of the model, i.e. with sums over lattice positions rather than integrals. In this case, however, there are extra terms which only become zero in the scaling limit. We have evaluate the integral in equation (7) numerically. As can be seen from figure 1, the fit to the simulation data is excellent. For small x expanding the exponential in equation (7) gives $C(x) = 1 - 2x + O(x^3)$. In fact, we can show directly that the small distance behaviour of the correlation function must have this form. Consider two-points separated by r spins. If P_I is the probability of finding an interface at a given site then for small P_I the probability of finding an interface between the two points is $P_I r$ and so the correlation function for these points is $C = 1 - 2P_I r$. However, the mean domain length is $L_0 = 1/P_I$ and so $C = 1 - 2r/L_0 = 1 - 2x$ for small x.

To derive equation (7) we assumed that large bonds would form barriers to interface movement irrespective of the size of the bonds between them. We believe that this assumption is correct for any unbounded distribution of bonds with a sufficiently broad tail. In the appendix we present an example calculation showing that this is indeed the case for an exponential distribution of bonds in the limit $L_0 \to \infty$. For power-law distributions, as we note in the appendix, the broader tail should ensure our treatment is valid.

We have used values of $\alpha = 1.3, 5.0$ and 10.0 as well as an exponential distribution in our simulations which all give excellent agreement with the calculated correlation function. This suggests that all distributions of bonds which have a probability density function non-zero at the smallest bond and unbounded from above have the same two-point correlation function. For a uniform distribution of bonds the situation is completely different, however, as the role of the minimum bond is as important as that of the large bonds. We now turn our attention to the calculation of the two-point correlation function for this bond distribution.

4.2. Uniform distribution of bonds

We now repeat the calculation for a uniform distribution of bonds. The idea is essentially the same as above in that we calculate the probability that there is no PI between two sites at a random location in the system separated by r spins. To do this, however, is rather more difficult as we must look at the differences between bonds instead of simply the largest bonds.

For the purposes of our algorithm the bonds can be taken to lie in $(0, 1)$ as only differences between bonds are relevant and changing the width of the distribution is equivalent to changing the temperature.

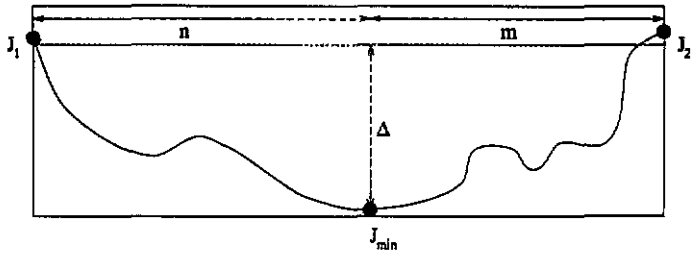

Figure 4. The configuration determining the mean domain length in the RBIM with a uniform distribution of bonds. The symbols are explained in the text.

We start by calculating the average domain scale L_0. Consider the situation shown in figure 4. $\Delta = 1 - \epsilon$ is the maximum energy barrier that has been jumped. J_1 and J_2 are the

first bonds to the left and right respectively of $J_{\min}$ with a value greater than $J_{\min}+\Delta$. For a PI to be at the site labelled by $J_{\min}$ we require $J_{\min}<\epsilon$, $J_1-J_{\min}>\Delta$ and $J_2-J_{\min}>\Delta$. Summing over all lengths n and m and integrating over all possible values of J_1, J_2 and $J_{\min}$ that are allowed by the above restrictions gives us the probability of a PI at a given site. In the scaling limit, Δ is very close to 1, so factors of Δ, Δ^2, etc, can be ignored. We therefore obtain the expression

$$\sum_{n=1}^{\infty}\sum_{m=1}^{\infty}\int_0^{1-\Delta} \mathrm{d}J\ \Delta^{n+m}(1-(J+\Delta))^2 \tag{8}$$

which, on evaluation of the integrals and sums, gives $(1-\Delta)/3$. The probability of finding an interface at a PI is $\frac{1}{2}$ so the average domain length is

$$L_0=\frac{6}{1-\Delta}\,. \tag{9}$$

There are three types of configuration which contribute to $C(x)$ in the scaling limit. We represent these schematically by the three diagrams shown in figure 5. The vertical scale corresponds to the bond strength and the horizontal scale to position. The points at the edge of the diagrams are the test points, separated by r spins, for which we are calculating the correlation function. Dotted lines denote regions of bonds which contain no barriers to interface motion; straight lines with an arrow represent regions where there are barriers but only in the direction opposite to the arrow. One can convince oneself after a little thought that all other diagrams containing a PI between the test points, have zero contribution in

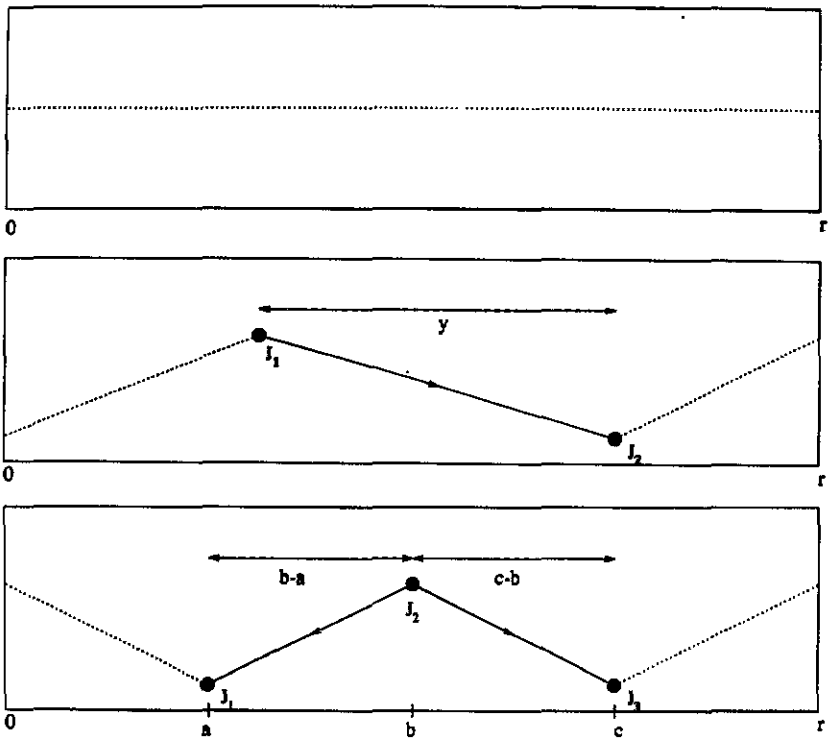

Figure 5. The three configurations contributing to the correlation function for the RBIM with a uniform distribution of bonds. The symbols are explained in the text.

the scaling limit or are already included as a subset of the diagrams in figure 5. These three diagrams therefore include all the necessary bond configurations. We will explain the diagrams in more detail below as we evaluate their contributions to $C(x)$.

The first diagram represents the situation where there are no barriers to interface motion between the test points. If $J_{\min}$ is the smallest of the bonds in this region then $J_{\min} > \epsilon$ implies there are no PIs. For $J_{\min} < \epsilon$ there could be a PI between the test points. We require that there be a bond smaller than $J_{\min}$ outside the spins and that the largest bond between this and the bond of size $J_{\min}$ is less than $J_{\min} + \Delta$. This ensures that an interface breaking the $J_{\min}$ bond is free to move to the smaller bond outside the test points.

The first case is simple. We integrate over all values of $J_{\min}$ and sum over all positions the least bond could occupy to get

$$\int_{\epsilon}^{1} \mathrm{d}J_{\min}\, r(1-J_{\min})^{r-1} = (1-\epsilon)^{r} \tag{10}$$

which in the scaling limit is $\exp(-r\epsilon) = \exp(-z)$ where $z = r\epsilon = r(1-\Delta) = 6r/L_0 = 6x$.

For the second case the condition that there is no larger bond than $J_{\min} + \Delta$ between $J_{\min}$ and the first smaller bond to the right, say, has probability

$$\sum_{n=0}^{\infty} \Delta^{n} J_{\min} = \frac{J_{\min}}{1-\Delta}. \tag{11}$$

We require this situation on the left, the right or both sides of the test points which has probability

$$1 - \left(1 - \frac{J_{\min}}{1-\Delta}\right)^{2} \tag{12}$$

hence we obtain the following expression for the contribution to the correlation function

$$\int_{0}^{\epsilon} \mathrm{d}J_{\min}\, r\Delta^{r-1}\left[1 - \left(1 - \frac{J_{\min}}{1-\Delta}\right)^{2}\right] \tag{13}$$

which becomes $(2/3)z\exp(-z)$ after evaluating the integrals and taking the scaling limit. The total contribution to $C(x)$ from the first diagram is therefore

$$C_1(z) = (1 + 2z/3)\exp(-z)\,. \tag{14}$$

We proceed in a similar fashion with the second diagram. The bond labelled J_1 is the largest bond between the test points and J_2 is the smallest. All bonds to the left of J_1 are smaller than J_1 but not so small so as to create a barrier. Similarly, all the bonds to the right of J_2 are larger then J_1 but not so large so as to create a barrier. The only bond that could possibly be a PI is J_2. To ensure that it is not we require, as before, that there is a bond less than J_2 to the right of the right test point with the bonds between this bond and J_2 all less than $J_2 + \Delta$. This has probability $J_2/(1-\Delta)$ as in equation (11). The bonds to the right of J_2 and the left of J_1 give a factor of Δ^{r-a}.

To complete the calculation we require the probability of the straight arrowed line in the second diagram. This line represents the situation where there are a bonds between two bonds of strength J_1 and J_2 which satisfy $J_1 - J_2 > \Delta$. In this region there are no barriers to left–right interface motion but there are an arbitrary number of right–left barriers present. To calculate the probability of such a configuration of bonds consider the situation shown in figure 6, which shows a possible bond configuration enclosed by the bonds J_1 and J_2.

We start by considering the bond strength $I_0 = J_1 - \Delta$. We find the first bond to the right that is smaller than I_0, I_1, say, at a distance a_1 from J_1. We then find the first smaller bond to the right of I_1 and continue this process until we reach the other side of the diagram. The last smaller bond we find, excluding J_2, is I_n at position a_n. By construction, J_2 is smaller than I_n and is at location $a_{n+1} \equiv a$. Now if all bonds between I_i and I_{i+1} are less than $I_i + \Delta$ for $0 < i < n+1$ then we see that the configuration generated cannot have any left–right barriers to interface motion. Futhermore, any configuration which does not have barriers to left–right interface motion can be constructed using the above procedure. Finally, we observe that each set of distinct variables $\{I_i, a_i\}$ generates distinct bond configurations hence the set of all $\{I_i, a_i\}$ covers all possible bond configurations that have no left–right barriers. To calculate the probability P_{LR} of no left–right interface barriers we therefore take the probability of a particular configuration, such as the one in figure 6, sum over all values of n and integrate over all allowed values of I_i and a_i. The probability density associated with figure 6 is simply $\Delta^{a-n} \prod_{i=1}^{n} dI_n da_n$. We therefore have

$$P_{LR}(a, J_1, J_2) = \sum_{n=0}^{\infty} \int_0^a da_1 \int_{a_1}^a da_2 \ldots \int_{a_{n-1}}^a da_n \int_{J_2}^{I_0} dI_1 \int_{J_2}^{I_1} dI_2 \ldots \int_{J_2}^{I_{n-1}} dI_n \, \Delta^{a-n}$$

$$= \sum_{n=0}^{\infty} \frac{\Delta^{a-n}(J_1 - J_2 - \Delta)^n a^n}{(n!)^2} . \tag{15}$$

Summing over n includes the possibility of any number of jumps. The resulting expression is

$$P_{LR}(a, J_1, J_2) = \Delta^a I_0\left(2\sqrt{a\left(\frac{J_1 - J_2}{\Delta} - 1\right)}\right) \tag{16}$$

where $I_0(z)$ is the modified Bessel function.

Using this expression we can now calculate the second diagram of figure 5. We integrate over all the allowed values of J_1 and J_2, integrate over all lengths a between J_1 and J_2 and include a factor $r - a$ for the possible positions of J_1. This gives us the expression

$$C_2(z) = \int_{\Delta}^{1} dJ_1 \int_0^{J_1 - \Delta} dJ_2 \int_0^r da\,(r-a)\Delta^a I_0\left(2\sqrt{a(\frac{J_1 - J_2}{\Delta} - 1)}\right)\Delta^{r-a}\frac{J_2}{1-\Delta} \tag{17}$$

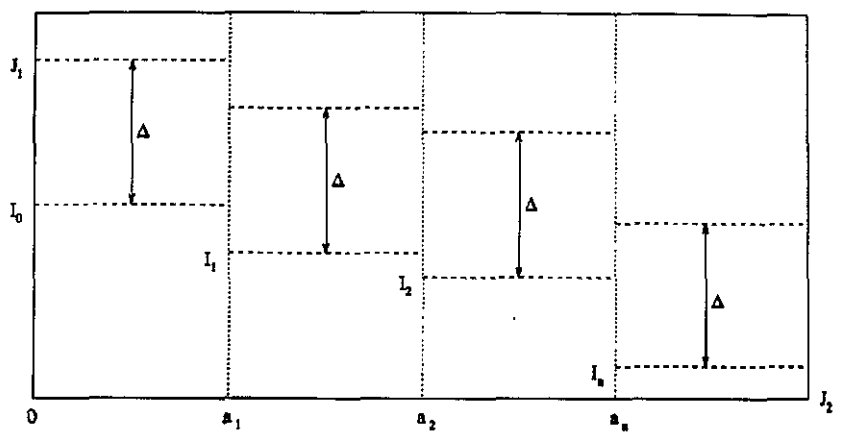

Figure 6. The configuration of bonds giving a right–left barrier to interface motion. See the text for details.

which can be evaluated by rewriting the Bessel function as a series as in equation (15), evaluating the integrals and resumming the resulting expression. This gives, after a little algebra

$$C_2(z) = 2z^2 e^{-z}\left[\frac{I_1(2\sqrt{z})}{\sqrt{z}} - \frac{z}{2} - 1\right] \tag{18}$$

where we have included an extra factor of 2 because the mirror image of diagram 2 gives the same contribution.

The procedure to evaluate diagram 3 is identical. This time we include a factor of P_{LR} for each of the arrowed lines. We also include two factors of the form of equation (11), which arise from the conditions that interfaces at the bonds J_1 and J_3 must be free to move to smaller bonds outside the test points. We integrate over J_1, J_2 and J_3 as well as the positions a,b and c. The resulting expression is

$$C_3(z) = \int_\Delta^1 dJ_2 \int_0^{J_2-\Delta} dJ_1 \int_0^{J_2-\Delta} dJ_3 \int_0^r dc \int_0^c db \int_0^b da \, \frac{J_1 J_3}{(1-\Delta)^2}\Delta^r I \tag{19}$$

where

$$I = I_0\left(2\sqrt{(b-a)\left(\frac{J_2-J_1}{\Delta}-1\right)}\right) I_0\left(2\sqrt{(c-b)\left(\frac{J_2-J_3}{\Delta}-1\right)}\right) \tag{20}$$

which when we take the scaling limit we can write in the form

$$C_3(z) = z^3 e^{-z} \int_0^1 dJ_1 \int_0^1 dJ_2 \int_0^1 dJ_3 \, J_1 J_3 J_2^4 \int_0^1 da \int_0^1 db \int_0^1 dc \, bc^2 I' \tag{21}$$

where now

$$I' = I_0\left(2\sqrt{abcJ_2(1-J_1)z}\right) I_0\left(2\sqrt{c(1-b)J_2(1-J_3)z}\right). \tag{22}$$

This integral can then be computed numerically. Our resulting expression for the correlation function including all the above contributions and replacing z by $6x$ is therefore

$$\begin{aligned} C(x) &= [A_1(x) + A_2(x)]\exp(-6x) \\ A_1(x) &= 1 + 4x + 12x\sqrt{6x} I_1(2\sqrt{6x}) - (6x)^3 - 72x^2 \\ A_2(x) &= (6x)^3 \int_0^1 dJ_1 \int_0^1 dJ_2 \int_0^1 dJ_3 \int_0^1 da \int_0^1 db \int_0^1 dc \, J_1 J_2^4 J_3 bc^2 A' \\ A' &= I_0\left(\sqrt{24abc(1-J_1)J_2x}\right) I_0\left(\sqrt{24(1-b)c(1-J_3)J_2x}\right). \end{aligned} \tag{23}$$

Figure 2 shows this function and the data from the numerical simulation. Once again, the agreement is excellent. In the scaling regime, the bonds that control interface motion are those very close to 0 and 1. We expect, therefore, that any bond distribution which is the same as the uniform distribution close to these values should give the same correlation function. Simulations with such bond distributions do, to within statistical errors, give correlation functions fitted by equation (23). A generalisation to arbitrary non-uniform distributions, however, would be difficult, mainly due to the problems in calculating P_{LR}.

5. The autocorrelation function

Another quantity of interest in the study of phase ordering dynamics is the autocorrelation function $C_0(t,t') = \langle S(i,t)S(i,t')\rangle$ where $S(i,t)$ is the value of the spin at site i and time

t. This is expected to have the scaling form $C_0(t, t') = g(L(t')/L(t))$ for large $L(t)$ and $L(t')$ with $t' > t$. As noted above, it is convenient to use the mean domain length to define the time scale. Hence we look at the quantity $A(L_1, L_2) = h(L_2/L_1)$.

For the two-point correlation function we were able to deduce the domain structure for large values of L_0 and hence the calculation of $f(x)$ was reduced essentially to a problem in combinatorics. For a very broad unbounded distribution of random bonds we can follow the same procedure for the autocorrelation function. Firstly, consider the system when it has evolved to a stage where the mean domain scale is L_1. The strong bonds, say those with strengths greater than J_1, occur with probability P_1 and confine the interfaces hence there is either zero or one interfaces between each pair of strong bonds. Let us refer to this state as the initial state. At a later stage of domain growth, defined by the length scale L_2, the strong bond strength J_2 and strong bond probability P_2, a fraction of the bonds which used to be nominated as strong bonds will no longer be so. Hence interfaces previously confined by them will be free to annihilate or move to positions with a lower energy. We refer to this state as the final state.

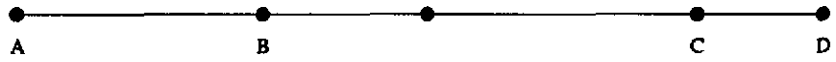

Figure 7. Configuration of strong bonds contributing to the autocorrelation function in the RBIM with an unbounded distribution of bonds. See the text for details.

To calculate the autocorrelation function we consider a region of N bonds between two bonds greater than J_2 with all the intervening bonds less than J_2. For all the possible configurations of bonds and positions of interfaces in the initial state, the domain structure of the final state can be inferred directly. If the initial number of interfaces is even then the final state will contain no interfaces whereas if the initial number is odd then there will be a single interface in the final state occupying the weakest of the N bonds. Now, consider the situation shown in figure 7. The bonds A and D are strong bonds in the final state, while the other strong bonds in between are only nominated as strong bonds in the initial state. The bond B is the first strong bond (in the initial state) to the right of A and the bond C is the first strong bond to the left of D. We now claim that after averaging over all positions B and C can occupy and over all possible initial interface positions the region BC gives no contribution to the autocorrelation function. To see why this is so consider a given set of bonds in AD. The final configuration is dependent only on the parity of the initial number of interfaces. Two initial configurations differing by the parity of the number of interfaces in AB and the parity of the number of interfaces in CD will therefore evolve to the same final configuration. Each of the spins in the region BC in one of these initial configurations is opposite in sign to the same spin in the other configuration, so the contributions BC gives to the autocorrelation function from the two configurations cancel. All initial configurations can be paired in this way so the net contribution from BC is zero.

The entire contribution to the autocorrelation function comes from the two regions AB and CD in figure 7. Consider for the moment just the region AB, as the contribution from CD is, by symmetry, the same. Suppose that in the final state there is no interface in AB. If there is also no interface in AB initially, then the contribution to the autocorrelation function from AB is the number of spins contained in it, i.e. a. Finally, if there is an interface in AB initially, however, then there is no net contribution because the interface is equally likely to lie anywhere in AB. Similarly, if there is an interface in AB in the final state but not in the initial state then there is no contribution to the autocorrelation function. If there is an interface in AB in both the initial and final states, then it must be at the same place in AB

(the weakest bond) and so the contribution to the autocorrelation function is the number of spins in AB again. Regardless of the final state, then, the contribution from AB is zero or a depending upon whether there is an interface in AB initially. The average contribution from AB and CD together is therefore $(a+b)/2$.

The value of the autocorrelation function in a region such as that shown in figure 7 is $(a+b)/(2N)$. The probability density of finding such a region is simply $P_M^2 \exp(-P_M(a+b))$, where P_M is the probability density of finding a bond $J > J_1$ given that $J < J_2$. It can easily be shown, using elementary probability theory, that $P_M = (P_1 - P_2)/(1 - P_2)$. In the scaling limit, $P_1 \to 0$, $P_2 \to 0$, P_1/P_2 arbitrary, $P_M = P_1 - P_2$. The expected value of the autocorrelation function from a region of N spins bounded by two bonds greater than J_2 and with at least two bonds greater than J_1 between these is therefore

$$A_1 = \int_0^N \mathrm{d}a \int_0^{N-a} \mathrm{d}b \; P_M^2 \exp(-P_M(a+b)) \frac{a+b}{2N}. \tag{24}$$

In addition to the configurations of the type shown in figure 7, there are two other configurations which contribute to the autocorrelation function. Firstly, there could be no strong bonds within the N spins, in which case the autocorrelation function is 1 within this region, hence the contribution is

$$A_2 = \exp(-N P_M) . \tag{25}$$

Secondly there could be a single strong bond, in which case the autocorrelation function can be evaluated exactly as above and takes the value

$$A_3 = \int_0^N \mathrm{d}a \; \frac{P_M \exp(-N P_M)}{2} . \tag{26}$$

The integrals in equations (24) and (26) can be evaluated straightforwardly and one finds the total expected contribution to the autocorrelation function A_T to be

$$A_T = A_1 + A_2 + A_3 = \frac{1 - \exp(-N P_M)}{N P_M} . \tag{27}$$

To calculate the full autocorrelation function we integrate over all N and weight the contribution from a region of length N by the probability of finding N bonds less than J_2 separating two bonds greater than J_2 and by a factor of N, which is included because the region contains N spins, each of which has an equal weight in the autocorrelation function. The resulting expression is therefore

$$A(P_1, P_2) = \int_0^\infty \mathrm{d}N \; N P_2^2 \exp(-N P_2) A_T \tag{28}$$

which, after evaluating the integrals and replacing P_M with $P_1 - P_2 = 2/L_1 - 2/L_2$, becomes

$$A(L_1, L_2) = \frac{L_1}{L_2} . \tag{29}$$

We have also measured this quantity in our simulations. We used a power-law distribution of bonds given by the probability density function $P(J) = (\alpha - 1)J^{-\alpha}$ where J lies in the interval $(1, \infty)$. The data are presented in figure 8, where we see that agreement with the theory is excellent for $\alpha = 1.2$. For larger values of α, however, the numerically determined scaling function moves away from the analytical form, in contrast to the situation for the two-point correlation function where all values of α gave the same scaling function.

In the case of the autocorrelation function we can see that the simplifying assumption of considering only the strong bonds and ignoring fluctuations in the size of the minimum bond between them is valid only for very broad distributions of bonds, i.e. for $\alpha \to 1$. This is because we have introduced two sets of strong bonds so that bonds belonging to the weaker set are automatically less than a given value, hence more likely to be effected by a large minimum bond.

The autocorrelation function has also been calculated for the $d = 1$ Glauber model [4]. In the scaling regime, at zero temperature, one finds

$$A(t_1, t_2) = \frac{2}{\pi} \sin^{-1}\left(\sqrt{\frac{2t_1}{t_2 + t_1}}\right). \tag{30}$$

For this model, $r \sim t^{1/2}$ and so the autocorrelation function has the same tail behaviour $A(L_1, L_2) \sim L_1/L_2$. The value of the exponent λ which characterizes the tail behaviour [10] is therefore not affected by the disorder, provided we write the autocorrelation function in terms of the lengths L_1 and L_2 rather than the times t_1 and t_2

We have also determined numerically the autocorrelation function for a uniform distribution of bonds. In this case the scaling function is different again, as it was for the two-point correlation function.

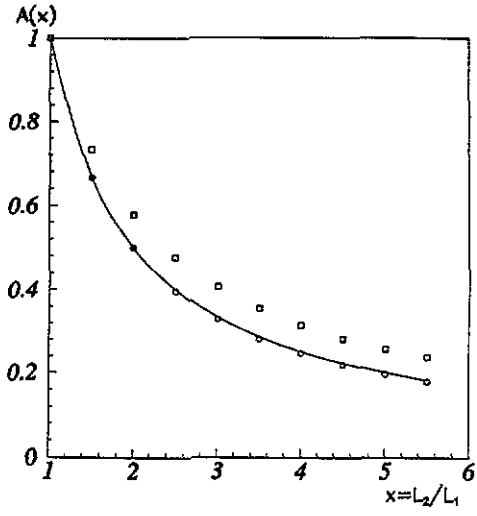

Figure 8. Scaling function for the autocorrelation function of the one-dimensional random-bond Ising model with a power-law distribution of bonds as defined in the text. The solid line is the analytical prediction and the data points come from a numerical simulation of 50 realizations of 10^5 spins. The data were taken using an initial domain size $L_1 = 200$. The circles are the data for $\alpha = 1.2$ and the squares the data for $\alpha = 3.0$.

6. Discussion and summary

We have introduced a model of domain growth in disordered systems which can be used to find exact forms for the two-point correlation function and autocorrelation function of the $d = 1$ random-bond Ising model for a range of disorder types. In these cases the dynamic scaling hypothesis has been explicitly demonstrated to hold. Systems with different unbounded distributions of bonds are found to belong to the same universality class, to the extent that the two-point correlation function is the same, but systems with uniform distribution of bonds belong to a different class. The autocorrelation function has been calculated for the limit of a very broad power-law distribution of bonds and has the same value of the exponent λ as the pure Glauber model. Other distributions of bonds give

different scaling functions for this correlation function however. In all cases the form of the correlation function is found to differ from that of the pure $d = 1$ Ising model.

So far we have not discussed how the characteristic scale $L(t)$ (defined as, say, the mean domain length L_0) depends on the time t of an underlying microscopic dynamics. The connection is simply made by equating the elapsed time t to the Arrhenius activation time for the dominant activation barriers Δ at length scale L_0, i.e. $t \sim \tau \exp\{\Delta(L_0)/T\}$, where τ is a microscopic time scale. Consider, for example, an unbounded $P(J)$. As usual, $L_0 = 2/P_S$, where P_S is the fraction of 'strong bonds'. For large L_0, the barrier $\Delta(L_0)$ is dominated by the strength J_S of the weakest strong bonds, defined by $P_S = \int_{J_S}^{\infty} \mathrm{d}J\ P(J)$. Thus $\Delta \simeq J_S \simeq T \ln(t/\tau)$ gives, ignoring constants of order unity,

$$L_0 \sim \left[\int_{T\ln(t/\tau)}^{\infty} \mathrm{d}J\ P(J)\right]^{-1}. \tag{31}$$

As explicit examples, we consider distributions with exponential and power-law tails, $P(J) \sim \exp(-J/J_0)$, and $P(J) \sim J^{-\alpha}$ respectively, for $J \to \infty$. These give $L_0 \sim t^{T/J_0}$ and $L_0 \sim (T \ln t)^{\alpha-1}$, respectively. For the uniform distribution of section 4.2, (9) gives $L_0 \sim [1 - \Delta]^{-1} \sim [1 - T \ln(t/\tau)]^{-1}$. While this formally gives an L_0 which diverges in finite time, one must remember that all our results are limited to the time regime where $L_0 \ll \xi(T)$, in which $\xi(T)$ is the equilibrium correlation length at temperature T. Otherwise one cannot ignore the effect of thermally activated domain walls.

For $d > 1$, domain growth in the Ising model is driven by the curvature of the domain walls. Because the introduction of disorder roughens these walls only as $W \sim L^{\zeta}$, where W is the typical fluctuation size induced in a domain wall of length L and ζ is an exponent less than 1 for all $d > 1$, on sufficiently large length scales the domain walls appear smooth. It is expected, therefore, that the two-point correlation function should not be effected by the introduction of disorder for $d > 1$ [10]. For $d = 1$, however, there is no curvature to drive the domain walls, so it is quite possible that the disorder may have some effect on the correlation functions, as indeed we have found in our model.

It should also be possible to calculate the two-point correlation function for the $d = 1$ random-bond Ising model with a conserved order parameter, or for the random field Ising model, within the framework of our model. Unfortunately, however, a generalization of the model to d greater than 1, where domain wall curvature would become important, does not seem possible.

Acknowledgment

RB thanks the SERC for a Research Studentship.

Appendix

In this appendix we consider a configuration in which the minimum bond between two strong bonds, i.e. bonds greater than J_S, is sufficiently large to allow an interface to pass over one of these bonds and show that for an unbounded distribution the probability of this configuration becomes zero in the limit of large domain scales.

Let us for simplicity take an exponential distribution of bonds. The probability density function is

$$P(J) = \alpha \mathrm{e}^{-\alpha J} \tag{A1}$$

where J lies in the interval $(0, \infty)$. The probability of finding a strong bond at a given site is therefore

$$P_S = \int_{J_S}^{\infty} \mathrm{d}J\ P(J) = \mathrm{e}^{-\alpha J_S} = \frac{2}{L_0} \tag{A2}$$

where J_S is the minimum size of a strong bond. Suppose we select a site at random in the system at a time when the mean domain length is L_0. Denote by a the number of weak bonds to the left of this site before a strong bond of size J_1 and by b the number of weak bonds to the right before another strong bond of size J_2. If the smallest of the weak bonds is of size $J_{\min}$ then the strong bonds fail to confine an interface on this bond if either J_1 or J_2 is less than $J_S + J_{\min}$.

The probability density for this configuration of bonds, correct to leading order in P_S, is

$$P_W(J_{\min}, a, b) = 2(a+b)P_S P(J_{\min})\left[\int_{J_{\min}}^{J_S} \mathrm{d}K\ P(K)\right]^{a+b-1} \int_{J_S}^{J_S+J_{\min}} \mathrm{d}K\ P(K)$$

$$= 2(a+b)\alpha P_S \mathrm{e}^{-\alpha J_{\min}}\left[\mathrm{e}^{-\alpha J_{\min}} - \mathrm{e}^{-\alpha J_S}\right]^{a+b-1}\left[\mathrm{e}^{-\alpha J_S} - \mathrm{e}^{-\alpha(J_S+J_{\min})}\right] \tag{A3}$$

where $P(J)$ is given by equation (A1). We now integrate over all possible values of a, b and $J_{\min}$ to find the total probability P_T of such a configuration. Using (A2) and the substitution $K = \mathrm{e}^{-\alpha J_S}$ we have

$$P_T = 2\int_0^{\infty} \mathrm{d}a \int_0^{\infty} \mathrm{d}b \int_0^{J_S} \mathrm{d}J_{\min}\ P_S^2 \alpha(a+b)\mathrm{e}^{-\alpha J_{\min}}\left(1 - \mathrm{e}^{-\alpha J_{\min}}\right)\left(\mathrm{e}^{-\alpha J_{\min}} - \mathrm{e}^{-\alpha J_S}\right)^{a+b-1}$$

$$= 2\int_0^{\infty} \mathrm{d}a \int_0^{\infty} \mathrm{d}b\ (a+b)P_S^2 \int_{P_S}^{1} \mathrm{d}K\ (1-K)(K-P_S)^{a+b-1}$$

$$= 2\int_0^{\infty} \mathrm{d}a \int_0^{\infty} \mathrm{d}b\ (a+b)P_S^2 \int_{P_S}^{1} \mathrm{d}K\ \left[(1-P_S)(K-P_S)^{a+b-1}\right.$$

$$\left. - (K-P_S)^{a+b}\right]$$

$$= 2\int_0^{\infty} \mathrm{d}a \int_0^{\infty} \mathrm{d}b\ \frac{P_S^2(1-P_S)^{a+b+1}}{a+b+1}$$

$$= 2P_S^2 \int_0^{\infty} \mathrm{d}r\ \frac{r(1-P_S)^{r+1}}{r+1} < 2P_S^2 \int_0^{\infty} \mathrm{d}r\ \mathrm{e}^{-rP_S} = 2P_S \tag{A4}$$

We therefore conclude that in the scaling limit, where $P_S \to \infty$, there are a negligible number of such regions and hence they do not alter the form of the two-point correlation function.

For bond probability density functions such as the exponential distribution or a power-law distribution, $J_{\min}$ will be very close the the minimum possible bond and hence insensitive to the precise form of the distribution. The arguments given above therefore depend only on the probability that a strong bond lies in the interval J_S to $J_S + \delta$, where δ is the difference between $J_{\min}$ and the minimum possible bond. For a power-law distribution defined by the probability density function $P(J) = (\alpha - 1)J^{\alpha}\theta(J-1)$ this probability is therefore given

by

$$\frac{\int_{J_S}^{J_S+\delta} \mathrm{d}J\ (\alpha-1)J^{-\alpha}}{\int_{J_S}^{\infty} \mathrm{d}J\ (\alpha-1)J^{-\alpha}} = 1-\left(1+\frac{\delta}{J_S}\right)^{1-\alpha} = (\alpha-1)\delta P_S^{1/(\alpha-1)} \tag{A5}$$

for large J_S. We see that for decreasing values of α, which correspond to increasingly broad tails, the probability for a bond to lie in $(J_S, J_S+\delta)$ gets smaller and hence our approximation should be better at small values of L_0. Indeed, we have observed in our numerical simulations that for smaller values of α the scaling function is approached more rapidly.

References

[1] For reviews, see:
Gunton J D, San Miguel M and Sahni P S *Phase Transitions and Critical Phenomena* vol 8, ed C Domb and J L Lebowitz (New York: Academic) p 267
Binder K 1987 *Rep. Prog. Phys.* **50** 783
Furukawa H 1985 *Adv. Phys.* **34** 703

[2] Lifshitz I M and Slyozov V V 1961 *J. Phys. Chem. Solids* **59** 668
Huse D A 1986 *Phys. Rev.* B **34** 7845
Voorhees P W 1985 *J. Stat. Phys.* **38** 231
Bray A J 1989 *Phys. Rev. Lett.* **62** 2841

[3] Lifshitz I M 1962 *Zh. Eksp. Teor. Fiz.* **42** 1354 (Engl. transl. 1962 *Sov. Phys.–JETP* **15** 939)
Allen S M and Cahn J W 1979 *Acta Metall.* **27** 1085

[4] The 1D Glauber model can be solved exactly, and exhibits scaling:
Bray A J 1989 *J. Phys. A: Math. Gen.* **22** L67
Amar J G and Family F 1990 *Phys. Rev.* A **41** 3258
The non-conserved O(n) model can be solved for $n = \infty$ and also scales, see, e.g.:
Coniglio A and Zannetti M 1989 *Europhys. Lett.* **10** 575

[5] Kawasaki K, Yalabik M C and Gunton J D 1978 *Phys. Rev.* A **17** 455
Ohta T, Jasnow D and Kawasaki K 1982 *Phys. Rev. Lett.* **49** 1223
Mazenko G F 1989 *Phys. Rev. Lett.* **63** 1605; 1990 *Phys. Rev.* B **42** 4487

[6] Bray A J and Puri S 1991 *Phys. Rev. Lett.* **67** 2670
Toyoki H 1992 *Phys. Rev.* B **45** 1965
Bray A J and Humayun K 1992 *J. Phys. A: Math. Gen.* **25** 2191
Fong Liu and Mazenko G F 1992 *Phys. Rev.* B **45** 6989

[7] Huse D A and Henley C L 1985 *Phys. Rev. Lett.* **54** 2708

[8] For Monte Carlo studies of the non-conserved case with quenched disorder, see:
Bray A J and Humayun K 1981 *J. Phys. A: Math. Gen.* **24** L1185
Grest G S and Srolovitz D J 1985 *Phys. Rev.* B **32** 3014
Chowdhury D, Grant M and Gunton J D 1987 *Phys. Rev.* B **35** 6792
Chowdhury D and Kumar S 1987 *J. Stat. Phys.* **49** 855
Oh J H and Choi D I 1986 *Phys. Rev.* B **33** 3448
Chowdhury D 1990 *J. Physique* **51** 2681

[9] For cell dynamical simulations of quenched disorder, see:
Puri S, Chowdhury D and Parekh N 1991 *J. Phys. A: Math. Gen.* **24** L1087
Puri S and Parekh N 1992 *J. Phys. A: Math. Gen.* **25** 4127

[10] Fisher D S and Huse D A 1988 *Phys. Rev.* B **38** 373